

## Design, synthesis, in vitro urease inhibitory potentials and *in silico* molecular docking study of benzimidazole bearing thiosemicarbazides/sulfonamide Analogues

Abdullah Yahya Abdullah Alzahrani<sup>a</sup>, Bushra Adalat<sup>b</sup>, Hayat Ullah<sup>c,\*</sup>, Muhammad Taha<sup>d</sup>, Mohamed S. Othman<sup>e,f</sup>, Mohamed A. Fareid<sup>e,g</sup>, Azza M. Khaled<sup>e,h</sup>, Fazal Rahim<sup>b,\*</sup>

<sup>a</sup> Department of Chemistry, Faculty of Science and Arts, King Khalid University, Mohail Assir, Saudi Arabia

<sup>b</sup> Department of Chemistry, Hazara University, Mansehra 21300, Khyber Pakhtunkhwa, Pakistan

<sup>c</sup> Department of Chemistry, University of Okara, Okara 56130, Pakistan

<sup>d</sup> Department of clinical pharmacy, Institute for Research and Medical Consultations (IRMC), Imam Abdulrahman Bin Faisal University, P.O. Box 31441, Dammam, Saudi Arabia

<sup>e</sup> Basic Sciences Department, Deanship of Preparatory Year, University of Ha'il, Hail 2440, Saudi Arabia

<sup>f</sup> Faculty of Biotechnology, October University for Modern Science and Arts (MSA), Giza 12566, Egypt

<sup>g</sup> Botany and Microbiology Department, Faculty of Science, Al-Azhar University, Cairo 11651, Egypt

<sup>h</sup> National Institute of Oceanography and Fisheries, Alexandria, Egypt

### ARTICLE INFO

#### Keywords:

Synthesis  
Benzimidazole analogs  
Urease activity  
SAR  
Molecular docking

### ABSTRACT

The nickel-containing urease enzyme is responsible for the pathogenesis of hepatic coma, hepatic encephalopathy, urolithiasis, gastric and peptic ulcer. These enzymes also have a negative effect on the efficacy of soil nitrogen to produce crops. The urease enzyme inhibitors may be thought as a strategy for reducing the negative effects of ureolytic bacteria. The present study involves a novel approach to the synthesis benzimidazole thiosemicarbazides and sulphonamide derivatives as potent urease inhibitor. All the analogues exhibited good inhibition potential. Among the thiosemicarbazides series, the most potent were analogs **1 g** and **1 h** having an  $IC_{50} = 2.40 \pm 0.10$  and  $3.10 \pm 0.10$   $\mu$ M respectively. Among the sulphonamide series, the most potent analogs were **2f** and **2j** having an  $IC_{50} = 3.90 \pm 0.10$  and  $1.40 \pm 0.001$   $\mu$ M respectively. Structure activity relationship study shows that among the two series, the most potent analogs were those having electron-withdrawing groups. Molecular docking study was carried out to check the interactions between the synthesized compounds and the urease enzyme's active sites. Furthermore, to evaluate the stability of the most active compound in complex with the urease enzyme a total of 200 ns MD simulation was carried out. The MD simulation study revealed that the compound formed a more stable complex with the urease enzyme and remained stable throughout the 200 ns MD simulation. All Compounds were verified for cytotoxicity against 3T3 mouse fibroblast cell line and detected nontoxic.

### 1. Introduction

Urease (urea amidohydrolase EC 3.5.15) is a nickel containing metalloenzyme which catalyzes the hydrolysis of urea to ammonia and carbon dioxide. Urease is involved in the function of using urea as nitrogen source [1–3]. Urease is known to be one of the major causes of diseases induced by *Helicobacter pylori*, thus allow them to survive at low pH inside the stomach and thereby, play an important role in the pathogenesis of gastric and peptic ulcer, apart from cancer as well [1].

Urease is directly involved in the formation of infection stones and contributes to the pathogenesis of urolithiasis, pyelonephritis, and hepatic encephalopathy, hepatic coma and urinary catheter encrustation [4]. Due to the diverse functions of this enzyme, its inhibition by potent and specific compounds could provide an invaluable addition for treatment of infections, and secondary complexes such as pus formation, and ulcer caused by urease-producing bacteria [5].

Benzimidazole-based heterocycles are becoming more popular because the benzimidazole moiety is so important to many biological

\* Corresponding author.

E-mail addresses: [ayaanwazir366@gmail.com](mailto:ayaanwazir366@gmail.com) (H. Ullah), [fazalstar@gmail.com](mailto:fazalstar@gmail.com) (F. Rahim).

<https://doi.org/10.1016/j.molstruc.2023.136850>

Received 18 July 2023; Received in revised form 3 October 2023; Accepted 12 October 2023

Available online 13 October 2023

0022-2860/© 2023 Elsevier B.V. All rights reserved.

processes and because it can be seen as an important pharmacophore in drug development processes [6,7]. Benzimidazole has been linked with a wide range of biological activities, including proton pump inhibitors [8], anti-virals [9], anti-oxidants [10], anti-hypertensives [11], carbonic anhydrase inhibitors [12], phosphodiesterase inhibitors [13], anti-cancer [14], anti-glycation [15], anti-inflammatory [16], anti-urease [17], antifungal [18], antibacterial [19], antihelminthic [20] and antidiabetic [21].

Thiosemicarbazones exhibit various biological activities and have therefore attracted considerable pharmaceutical interest [22]. They have been evaluated over the last 50 years as antiviral, antibacterial and anticancer therapeutics. Thiosemicarbazones belong to a large group of thiourea derivatives, whose biological activities are a function of parent aldehyde or ketone moiety [23,24]. Conjugated N–N–S tridentate ligand system of thiosemicarbazide (NH<sub>2</sub>–CS–NH–NH<sub>2</sub>) seems essential for anticancer activity, possibly due to the observation that structural alterations that hinder a thiosemicarbazones ability to function as a chelating agent tend to destroy or reduce its medicinal activity [25].

Sulfonamide containing compounds got substantial attention from last few decades and emerged as potent inhibitor against varied disease including diabetes [26], psychosis [27], central nervous system (CNS) disorders [28], tumors [29] and different cancer treatments [30].

Recently, benzimidazole scaffolds were reported as  $\alpha$ -glucosidase inhibitors [31–33], sulfonamide as carbonic anhydrase inhibitors [34] and novel barbituric derivatives as potent urease inhibitors [35–37]. Our research group has recently reported benzimidazole Schiff base and thiosemicarbazones as potent anti-Alzheimer agents [38], 2-(2-pyridyl) benzimidazole as anti-urease agents [39], benzimidazole bis-Schiff base as  $\alpha$ -glucosidase inhibitors [40], and benzimidazole derivatives as  $\alpha$ -amylase inhibitors [41]. But still there is need to discover more potent analogs which can act as lead therapeutic agents. For this purpose, we synthesize benzimidazole analogue (III) upon reacting aromatic diamine with aromatic aldehyde. Then analogue (III) was treated with hydrazine hydrate to form hydrazide intermediate (IV). Intermediate (IV) was firstly reacted with aromatic isothiocyanates to yield analogues benzimidazole-based thiosemicarbazide analogues and secondly was

treated with aromatic sulfonamide chloride to yield benzimidazole-based sulfonamide analogues and screened them for their urease inhibitory potentials.

## 2. Results and discussion

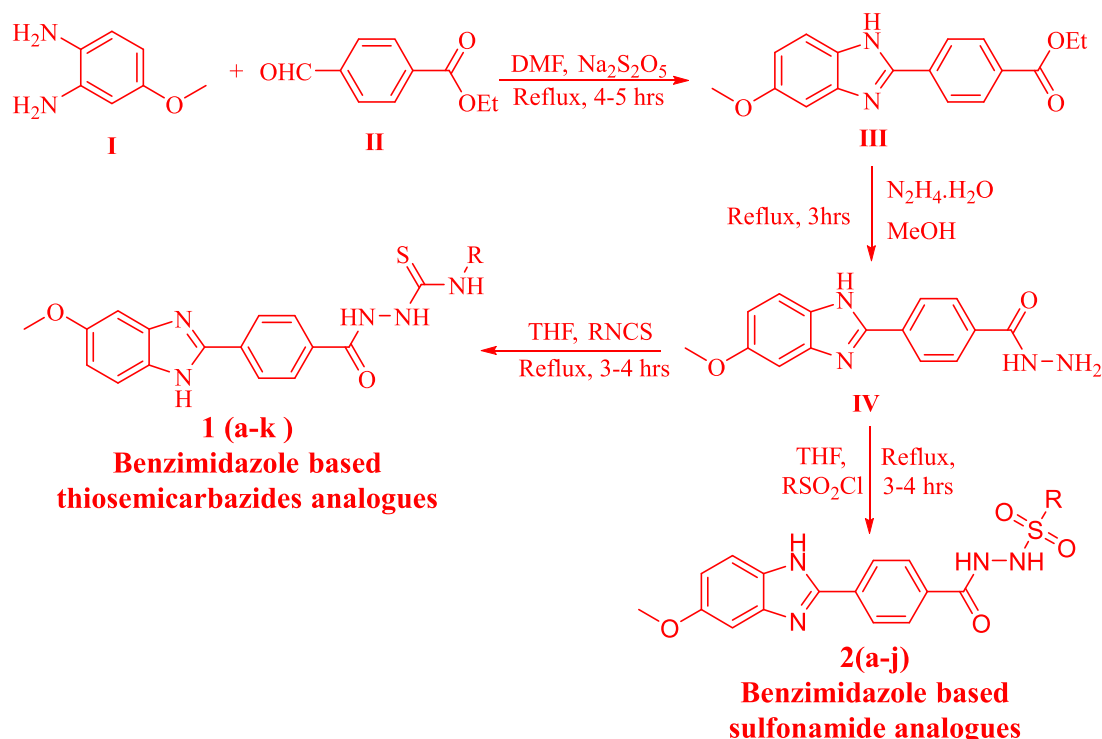
### 2.1. Chemistry

4-Methoxybenzene-1,2-diamin (I) reacted with ethyl-4-formyl benzoate (II) in DMF as solvent and sodium meta-bisulfite (Na<sub>2</sub>S<sub>2</sub>O<sub>5</sub>) was used as a base and refluxed for 4–5 h to obtain first intermediate product (III). Intermediate product (III) was then reacted with hydrazine hydrate and refluxed for 3 h to obtain the second intermediate product (IV). Finally the intermediate (IV) reacted in two different ways. Firstly, intermediated IV was reacted with differently substituted sulfonyl chloride in the presence of THF to yield benzimidazole- thiosemicarbazides hybrid analogues (1a–j) (Scheme 1, Table 2). Secondly intermediate IV was reacted with differently substituted isothiocyanate were reacted in the presence of THF to yield benzimidazole-sulfonamide (2a–k) (Scheme 1, Table 2).

### 2.2. Biological activity

#### 2.2.1. Urease inhibition activity of benzimidazole based thiosemicarbazides

We have synthesized of benzimidazole-based thiosemicarbazides analogs and inspected them for urease inhibitory potentials. All the analogs demonstrated well to moderate inhibition activities when compared with the standard drug thiourea (IC<sub>50</sub> = 21.60 ± 0.30  $\mu$ M). SAR studies show that all analogs having an electron withdrawing group on phenyl ring exhibited significant inhibition. The most potent analogs among the series were analogs 1 g (IC<sub>50</sub> = 2.40 ± 0.10  $\mu$ M), 1f (IC<sub>50</sub> = 4.60 ± 0.10  $\mu$ M), and 1 h (IC<sub>50</sub> = 3.10 ± 0.10  $\mu$ M). These analogs have halogen atom chlorine and bromine on the phenyl ring. The high activities of these analogs might be due to their high electronegativity values and size which allow the molecule to fit well in the active sites of enzyme. Contrary to this, analog 1b having bromine atom at 2 positions

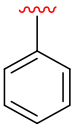
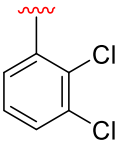
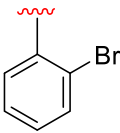
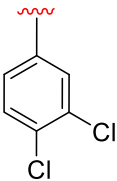
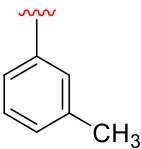
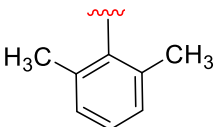
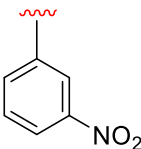
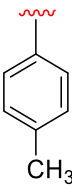
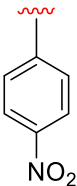
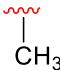
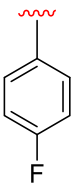


**Scheme 1.** Synthesis of benzimidazole bearing thiosemicarbazides/sulfonamide analogues.

on the phenyl ring exhibited weak inhibition with  $IC_{50}$  value of  $38.46 \pm 0.90 \mu\text{M}$ . So it is clear that the large size of bromine may cause difficulty in binding effectively with the enzyme active sites [43]. The unsubstituted analog **1k** was also a potent analog with  $IC_{50}$  value of  $4.90 \pm 0.10 \mu\text{M}$ . Obviously it gives an insight that the presence of substituent is

not important. It may be possible that the compound **1k** has such conformation which can fit well in the active site of the enzyme and block the activity. The next potent analogs among the series are analog **1d** and **1e** having electron-withdrawing nitro groups. The  $IC_{50}$  values of these analogs are  $18.60 \pm 0.50 \mu\text{M}$  and  $12.60 \pm 0.40 \mu\text{M}$ , respectively.

**Table 1**  
Different substituents and urease activity of benzimidazole-thiosemicarbazides analogues.

S. No	R	$IC_{50}$ Value	S. No	R	$IC_{50}$ Value
1a		$32.20 \pm 0.80$	1g		$2.40 \pm 0.10$
1b		$38.46 \pm 0.90$	1h		$3.10 \pm 0.10$
1c		$22.60 \pm 0.70$	1i		$17.30 \pm 0.10$
1d		$18.60 \pm 0.50$	1j		$22.80 \pm 0.50$
1e		$12.60 \pm 0.40$	1k		$4.90 \pm 0.10$
1f		$4.60 \pm 0.10$			
Thiourea		$21.60 \pm 0.30$			

The high inhibition activity of these analogs might be due to the chelating property of oxygen with the active sites of enzymes [44]. A slight difference in their values may be due to the position of the nitro group on the phenyl ring. Analogs **1c**, **1i**, and **1j** having methyl group on phenyl ring displayed inhibition almost comparable to standard drug thiourea. It is clear from **Table 1** that the difference in their values is due to the number and position of the methyl group on the phenyl ring. Analog **1a** having no substituent on the phenyl ring was weak in their inhibition activity with  $IC_{50}$  value of  $32.20 \pm 0.80 \mu\text{M}$ . This study revealed that the substitution of a functional group on phenyl ring employs a critical impact on urease inhibition.

### 2.2.2. Urease inhibition activity of benzimidazole-based sulphonamide derivatives

The synthesized benzimidazole sulphonamide derivatives were screened for urease inhibition activity. All the analogs exhibited varying degrees of urease inhibition activity. The sulphonamide derivatives exhibited lower inhibition activity than thiosemicarbazides. Structure-activity relationship shows that the electron withdrawing group on the phenyl ring plays a major role in inhibiting urease activity. Analog **2j** was found to be the most potent analog of the series having an  $IC_{50}$  value of  $1.40 \pm 0.001 \mu\text{M}$ . This analog has two fluorine atoms at positions 2 and 4. This shows that halogen atoms at the *ortho* and *para* position on the phenyl ring increase the urease inhibition activity. A comparison of analog **2a** and **2b** shows that analogs having mono-halogen atoms are less potent as compared to di-substituted analogs which are clear from the  $IC_{50}$  values given in **Table 2**. Similarly, among the chloro substituted analogs, analog **2c** in which the chloro group is at the *ortho* position is more potent having an  $IC_{50}$  of  $14.30 \pm 0.30$  as compared to analog **2d** in which the chloro group is at the *para* position having an  $IC_{50}$  value of  $16.40 \pm 0.30$ . Among the nitro substituted analogs **2e**, **2f**, and **2g**, the di-nitro analog **6** exhibited excellent urease inhibition having an  $IC_{50}$  value of  $3.90 \pm 0.10 \mu\text{M}$  while the mono-nitro analog **2e** ( $IC_{50} = 14.80 \pm 0.30 \mu\text{M}$ ) having the nitro group at *para* position showed moderate activity while analog **2g** ( $IC_{50} = 22.10 \pm 0.50 \mu\text{M}$ ) having *meta* nitro group was less potent. The rest of the analogs were poor in their inhibition activity.

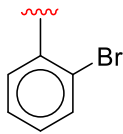
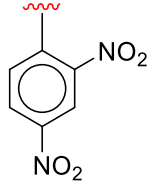
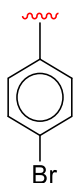
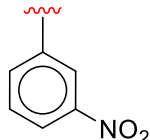
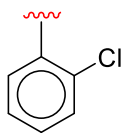
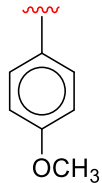
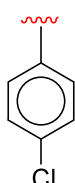
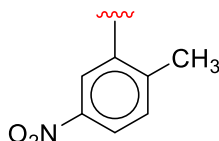
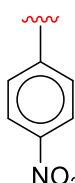
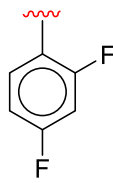
### 2.3. Molecular docking studies

#### 2.3.1. Molecular docking studies of benzimidazole bearing thiosemicarbazides analogs

Molecular docking analysis was conducted through MOE to show the binding interactions of the synthesized compounds against the urease enzyme. The most promising docking conformation for all compounds was established with accurate direction in the active site of the enzyme. The binding site of the enzyme is composed of both hydrophilic and hydrophobic amino acids as shown in **Fig. 1**. The two implanted Ni ions, i.e., Ni-798 & Ni-799 play a vital role by connecting the catalytic residue with the important moieties of the compound. According to the results of the molecular docking investigation, all the compounds displayed fit-well behavior in the active site of the urease enzyme.

Additionally, the most promising docked conformation of each compound was assessed further for binding mode analysis based on protein-ligand interaction (PLI) profile and docking score. In general, it was found from the post-docking study that the enlisted synthetic molecule had several substituted groups; some have electron withdrawing groups (EWG), while others have electron donating groups (EDG). Moreover, we've noticed that the enzyme activity was ultimately affected by the position, volume, and switching behavior of the substituted groups from EWG to EDG or vice versa. The high potency of compound **1g** was established from both in-vitro and PLI examinations. This investigation shows that compound **1g** adopts the most promising interactions with the critical residues. Both in-vitro and PLI research indicated that the most active compound **1g**, which has a high potency, is the only one in the series to adopt the most favorable interactions with the critical residues and with the two entrenched Ni ions i.e., **798** & **799**.

**Table 2**  
Structure and urease inhibition activities of benzimidazole based sulphonamide derivatives.

S. No	Structure	$IC_{50}$ values	S. No	Structure	$IC_{50}$ values
2a		30.60 $\pm 0.70$	2f		3.90 $\pm 0.10$
2b		28.20 $\pm 0.70$	2g		22.10 $\pm 0.50$
2c		14.30 $\pm 0.30$	2h		23.10 $\pm 0.50$
2d		16.40 $\pm 0.30$	2i		16.80 $\pm 0.40$
2e		14.80 $\pm 0.30$	2j		1.40 $\pm 0.001$
	Thiourea	21.60 $\pm 0.30$		Thiourea	21.60 $\pm 0.30$

These nickel ions show conjugation with the electron-withdrawing group of the compound and Ni-799 interacts with the three residues. The high inhibition activity of this compound is due to the electron-withdrawing group which extracts electron density from the conjugated system through resonance effect and thus making it less nucleophilic. The electron-withdrawing effect of these compounds also creates a partial positive charge on the benzene ring which then tend to stabilize itself by gaining or sharing electrons with the surrounding significant moieties as shown in **Fig. 1b**. Likewise other compounds in the series that demonstrated good inhibition against the urease enzyme have the

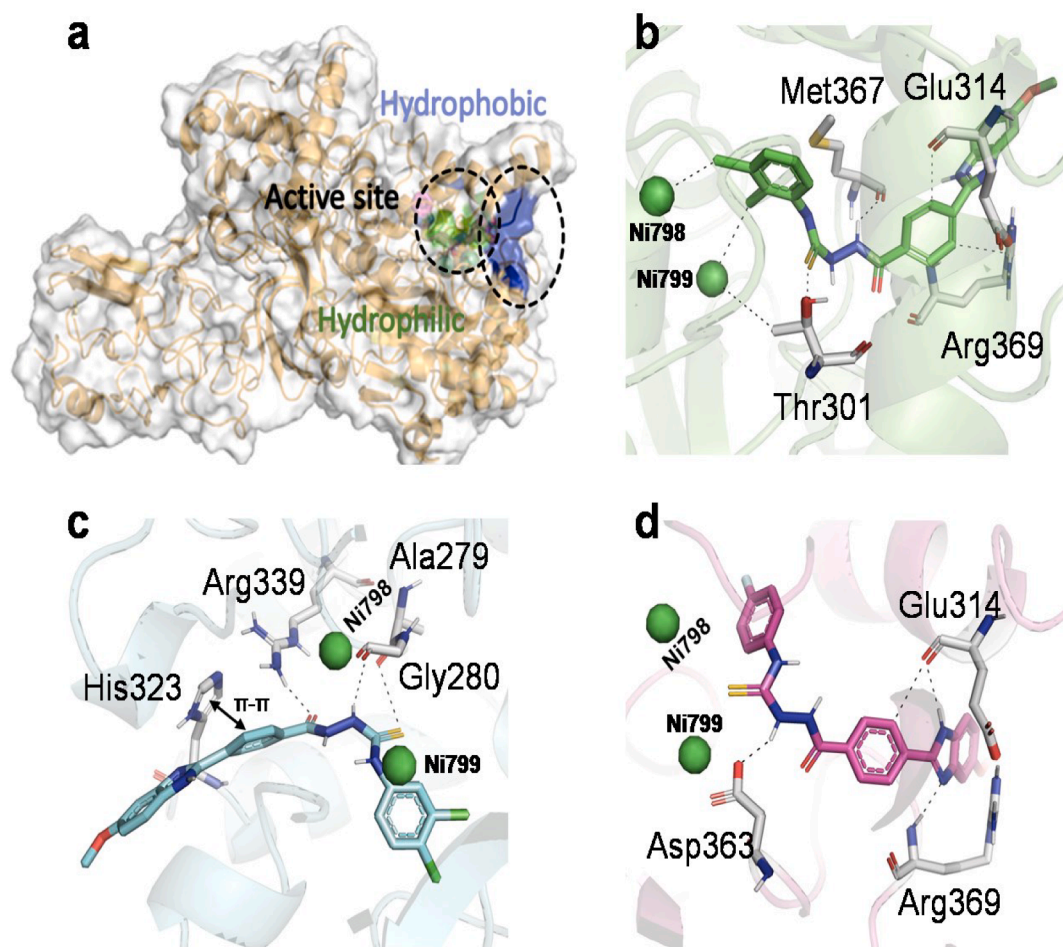


**Fig. 1.** The PLI profile for synthesized compounds against urease enzyme. (A) The surface representation of the urease enzyme. (B) The PLI pose for the most active compound 1 g, (C) for 1 h, and (D) for 1f. Dash lines indicate the H-bond while both-sided arrows indicate the pi-stacking interaction.

same electron withdrawing group but their position is different. So, it can be concluded that variation in the position of the functional group plays a major role in increasing or decreasing the inhibition activity. The PLI for ranked 2nd and 3rd has been embedded in Fig. 1c and d. Overall, we have concluded that the attachment position and the quantity does matter for the enzymatic activity of the targeted enzyme, as in the case of the compound 1 g and 1 h, which hold similar groups at different position.

### 2.3.2. Molecular docking studies of benzimidazole-bearing sulfonamide derivatives

A molecular docking study was conducted to demonstrate the binding mode of the synthesized analogs against the urease enzyme. The docking results showed that analogs have fit-well behavior of binding interactions in the active gorge of the enzyme with suitable location. Mostly, the active site of the urease enzyme contains both hydrophilic and hydrophobic residues. As illustrated in Fig. 2a, the hydrophobic site is made up of a group of surface residues (A170, 366, K169, L319, and C322), whereas the hydrophilic site is made up of residues (E166, 223, R339, D224, 494, H315, 323, 324, and H249), respectively. Furthermore, the two Ni ions (798 & 799) play a major in connecting the active sites of the enzyme with the important part of the compound. Additionally, the two embedded Ni ions (798 & 799) in combination play a significant role by linking the key active site residues with the compound's important moieties. More importantly, based on the protein-ligand interaction (PLI) profile, the most promising docked conformation of each compound was assessed further for binding mechanism. The synthesized analogs have different groups some possess electron-

withdrawing groups and some electro-donating groups, but it is clear from the results that compounds having electron withdrawing groups were more potent in their inhibition activities. The high potency might depend on the number of electrons-withdrawing groups and their electronegativity e.g., compound 2f and compound 2j both have electron withdrawing groups, but the high inhibition value of compound 2j might be due to the high electronegativity of fluorine. The key interactions of this compound with the important residues and with the Ni ions are shown in Fig. 2b. Their electronegativity difference and the PLI profile might be one of the reasons that ranked the compound having an F group superior to the N group as shown in Fig. 1c. The next potent compound (compound 2c) in the series which ranked 3rd also showed a good PLI profile as shown in Fig. 2d. Overall, we have observed and concluded that the compound holds the withdrawing group, and had a high electronegativity showing a high potential against the target enzyme. Other compounds which has donating also showed good inhibitory potential but comparatively less than the withdrawing group.

## 2.4. Post MD simulation analysis

### 2.4.1. Root mean square deviation (RMSD)

A high RMSD value indicates less stability of a system and lower RMSD value suggests stronger system stability [41]. The Urease/compound 2j system revealed an average RMSD value of 2.5 Å. The system revealed minor fluctuations during 20–40, 70–80 ns and 120–130 ns however no major deviations were observed during the entire 200 ns MD simulation. On the other hand, the control complex was found to be less stable as compared to the compound 2 J during MD

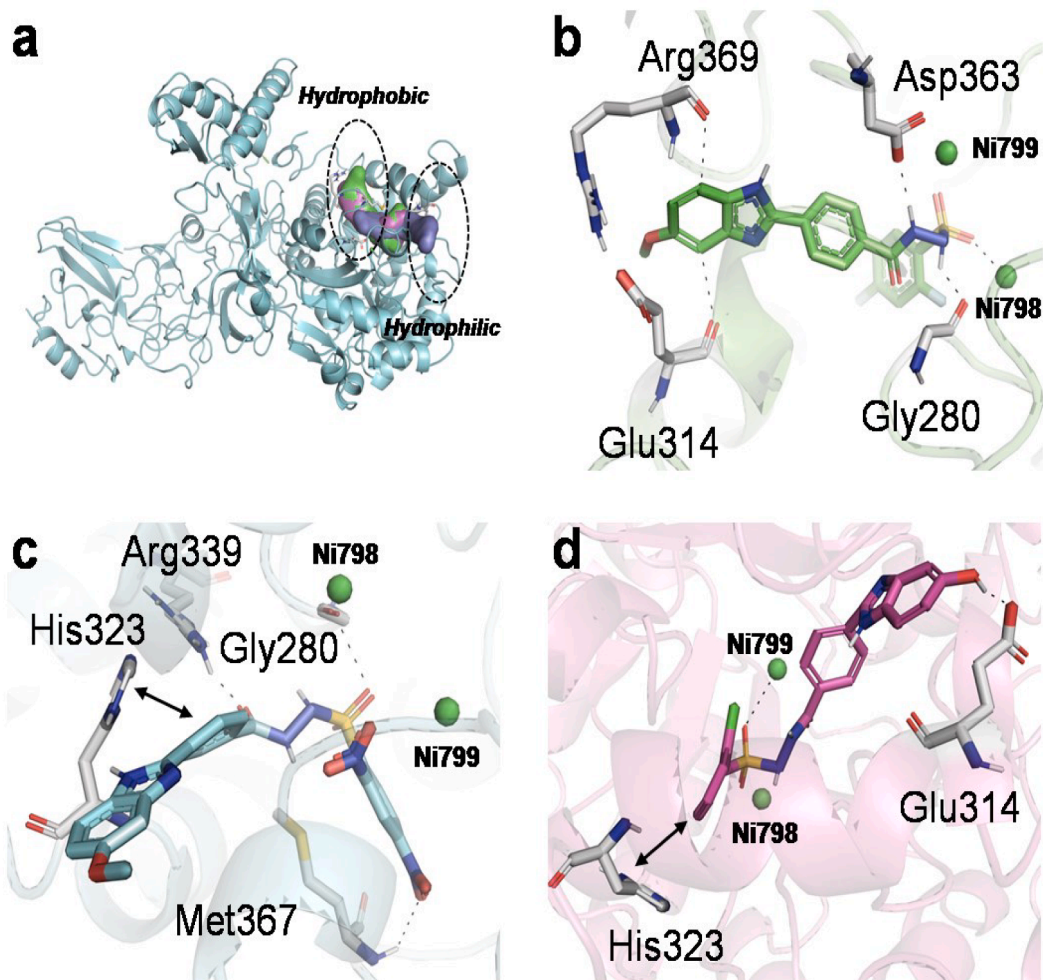


**Fig. 2.** The PLI profiling for potent compounds against the urease enzyme. (a) The cartonic representation of the urease enzyme. The hydrophobic and hydrophilic site has been encircled with dotted lines with labelled. (b) The PLI pose for the most active compound 2j, (c) for 2f, and (d) for 2c. Dash lines indicate the H-bond while both sided arrows indicate the pi-stacking interaction.

simulation. Initially the control system was stable during the first 30 ns after that some major fluctuations were observed till 130 ns and the complex revealed an unstable behavior. After 30 ns no major or minor deviations were observed till the 200 ns. From 130 ns the RMSD decreased to 3.4 Å and the system gained stability. Fig. 3 shows the RMSD plots for the control system in comparison with the compound 2j-urease complex.

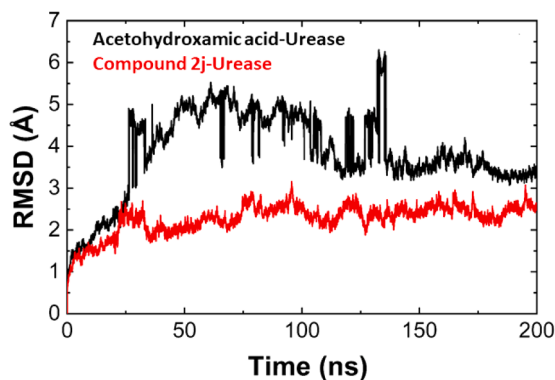


**Fig. 3.** RMSD analysis of acetohydroxamic acid-urease (Black), and Compound 2j-Urease (Red). The value of RMSD is displayed on the Y-axis and time in nano second is shown on X-axis.

#### 2.4.2. Root mean square fluctuation (RMSF)

We employed root mean square fluctuation (RMSF) analysis to identify the fluctuating regions in all four systems. Residues 20–30, 331–341, 461–469 had larger fluctuations and these residues revealed unstable behavior during MD simulation. The residues such as 100–335

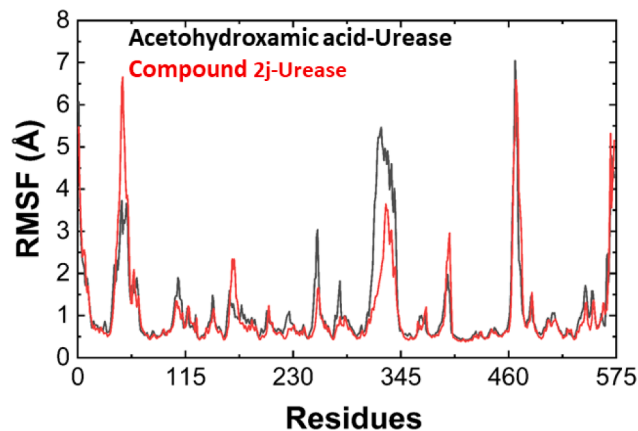


**Fig. 4.** RMSF analysis of acetohydroxamic acid-urease (Black), and Compound 2j-Urease (Red). The value of RMSF is displayed on the Y-axis and the number of residues are shown on X-axis.

and 345–460 and 475–575 revealed less fluctuations and a stable behavior during MD simulation. Fig. 4 display the RMSF plot of the protein-ligand complexes.

#### 2.4.3. Dynamics cross-correlation matrix (DCCM)

The dynamic cross-correlation map (DCCM) was generated to examine the inter-residues correlation. Throughout the MD simulation, strongly correlated (positive) and anti-correlated (negative) motions between the residues are depicted in red-yellow and dark-blue to light blue, respectively. The positive and negative correlation between the residues is seen in Fig. 5. Positively correlated motions were especially evident at the active site region, and a higher percentage of positive correlated residues in the compound 2j-Urease indicates that the compound is able to bind tightly to the target protein.

## 4. Conclusion

We design, synthesis, and bio-assay of benzimidazole bearing thiosemicarbazides and sulfonamide analogues with the goal of identifying more potent urease inhibitors. All of the compounds in both series inhibited urease well, with IC<sub>50</sub> values in the sub-micromolar range. Among the thiosemicarbazides series, the most potent are analogues **1 g** and **1 h** while among sulfonamide series, the most potent analogs are **2 f** and **2 j**. Molecular docking experiments were also used to find out the binding mechanisms of the synthesized analogues with the active site of enzymes. The most active compound was subjected to 200 ns MD simulation and the result was compared to the standard inhibitor. The more potent compound i.e. compound **2 j** revealed high stability during the 200 ns MD simulation.

### 4.1. Experimental

#### 4.1.1. General procedure for the synthesis of benzimidazole thiosemicarbazides analogs

4-Methoxybenzene-1,2-diamin (**I**) reacted with ethyl-4-formyl benzoate (**II**) in DMF as solvent and sodium meta-bisulfite (Na<sub>2</sub>S<sub>2</sub>O<sub>5</sub>) was used as a base and refluxed for 4–5 h to obtain first intermediate product (**III**). Intermediate product (**III**) was then reacted with hydrazine hydrate and refluxed for 3 h to obtain the second intermediate product (**IV**). Finally, the intermediate (**IV**) reacted in two different ways. Firstly, intermediated **IV** was reacted with differently substituted sulfonyl chloride in the presence of THF to yield benzimidazole- thiosemicarbazides hybrid analogues (**1 a-j**). Secondly intermediate **IV** was reacted with differently substituted isothiocyanate were reacted in the presence of THF to yield benzimidazole-sulfonamide (**2 a-k**).

### 4.2. Structural analysis

#### 4.2.1. 2-(4-(5-methoxy-1H-benzo[d]imidazol-2-yl)benzoyl)-N-phenylhydrazine-1-carbothioamide (**1a**)

<sup>1</sup>HNMR (500 MHz, DMSO-*d*<sub>6</sub>): 10.6 (s, 1H, NH), 10.5 (s, 1H, NH), 9.7 (s, 1H, NH), 9.6 (s, 1H, NH), 8.3 (d, *J* = 6.9 Hz, 2H, Aromatic H), 8.2 (m, 2H, Aromatic H), 8.1 (d, *J* = 6.4 Hz, 2H, Aromatic H), 7.7 (d, *J* = 6 Hz, 1H, Aromatic H), 7.6 (d, *J* = 6.2 Hz, 2H, Aromatic H), 7.3 (m, 2H, Aromatic H), 7.2 (d, *J* = 6.8 Hz, 1H, Aromatic H), 3.6 (s, 3H, OCH<sub>3</sub>); <sup>13</sup>CNMR (125 MHz, DMSO-*d*<sub>6</sub>): δ 183.6, 164.9, 156.4, 152.3, 139.2, 137.9, 137.9, 133.4, 132.5, 130.3, 130.2, 129.1, 129.0, 127.9, 127.7, 127.6, 126.5, 126.5, 119.6, 112.8, 78.3, 66.8. HREI-MS: *m/z* calcd for C<sub>22</sub>H<sub>19</sub>N<sub>5</sub>O<sub>2</sub>S, [M]<sup>+</sup> 417.1259; Found: 417.1250.

#### 4.2.2. N-(2-bromophenyl)-2-(4-(5-methoxy-1H-benzo[d]imidazol-2-yl)benzoyl)hydrazine-1-carbothioamide (**1b**)

<sup>1</sup>HNMR (500 MHz, DMSO-*d*<sub>6</sub>): 8.3(m, 2H, Aromatic H), 8.1(d, *J* = 6.5 Hz, 2H, Aromatic H), 7.9 (d, *J* = 6.8 Hz, 1H, Aromatic H), 7.8 (t, *J* = 6.8 Hz, 1H, Aromatic H), 7.6 (m, 2H, Aromatic H), 7.5 (m, 1H, Aromatic H), 7.3 (d, *J* = 6.3 Hz, 2H, Aromatic H), 3.6 (s, 3H, OCH<sub>3</sub>); <sup>13</sup>CNMR (125 MHz, DMSO-*d*<sub>6</sub>): δ 183.4, 165.6, 156.8, 152.0, 139.0, 137.6, 136.8, 132.6, 132.4, 132.3, 132.0, 131.8, 130.0, 130.0, 128.3, 127.7, 127.6, 121.4, 120.0, 112.1, 74.5, 67.0. HREI-MS: *m/z* calcd for C<sub>22</sub>H<sub>18</sub>BrN<sub>5</sub>O<sub>2</sub>S, [M]<sup>+</sup> 495.1259; Found: 495.0353.

#### 4.2.3. 2-(4-(5-methoxy-1H-benzo[d]imidazol-2-yl)benzoyl)-N-(*m*-tolyl)hydrazine-1-carbothioamide (**1c**)

<sup>1</sup>HNMR (500 MHz, DMSO-*d*<sub>6</sub>): 10.6 (s, 1H, NH), 10.3 (s, 1H, NH), 9.7 (s, 1H, NH), 8.7 (s, 1H, NH), 8.3 (d, *J* = 6.9 Hz, 2H, Aromatic H), 8.1 (d, *J* = 6.0 Hz, 2H, Aromatic H), 7.7 (t, *J* = 6.1 Hz, 1H, Aromatic H), 7.6 (d, *J* = 6.9 Hz, 1H, Aromatic H), 7.5 (m, 1H, Aromatic H), 7.4 (m, 2H, Aromatic H), 7.0 (d, *J* = 6.2 Hz, 2H, Aromatic H), 3.6 (s, 3H, OCH<sub>3</sub>), 2.3 (3H, OCH<sub>3</sub>); <sup>13</sup>CNMR (125 MHz, DMSO-*d*<sub>6</sub>): δ 184.2, 164.7, 156.5, 153.2, 139.6, 139.1, 138.4, 137.4, 134.4, 132.0, 130.5, 130.4, 128.5, 127.2, 127.2, 126.4, 124.8, 123.6, 118.9, 112.2, 92.6, 66.7, 20.9. HREI-MS: *m/z* calcd for C<sub>23</sub>H<sub>21</sub>N<sub>5</sub>O<sub>2</sub>S, [M]<sup>+</sup> 431.1416; Found: 431.1411.

#### 4.2.4. 2-(4-(5-methoxy-1H-benzo[d]imidazol-2-yl)benzoyl)-N-(3-nitrophenyl)hydrazine-1-carbothioamide (**1d**)

<sup>1</sup>HNMR (500 MHz, DMSO-*d*<sub>6</sub>): 10.73 (s, 1H, NH), 10.64(s, 1H, NH), 10.1 (s, 1H, NH), 9.1 (s, 1H, NH), 8.5 (s, 1H, Aromatic H), 8.3 (d, *J* = 6.8 Hz, 2H, Aromatic H), 8.2 (m, 3H, Aromatic H), 8.1 (t, *J* = 7 Hz, 1H, Aromatic H), 7.7 (t, *J* = 6.1 Hz, 2H, Aromatic H), 7.4 (d, *J* = 6.4 Hz, 1H, Aromatic H), 7.2 (d, *J* = 6.7 Hz, 1H, Aromatic H), 3.6 (s, 3H, OCH<sub>3</sub>); <sup>13</sup>CNMR (125 MHz, DMSO-*d*<sub>6</sub>): δ 183.9, 165.2, 156.5, 153.1, 150.2,

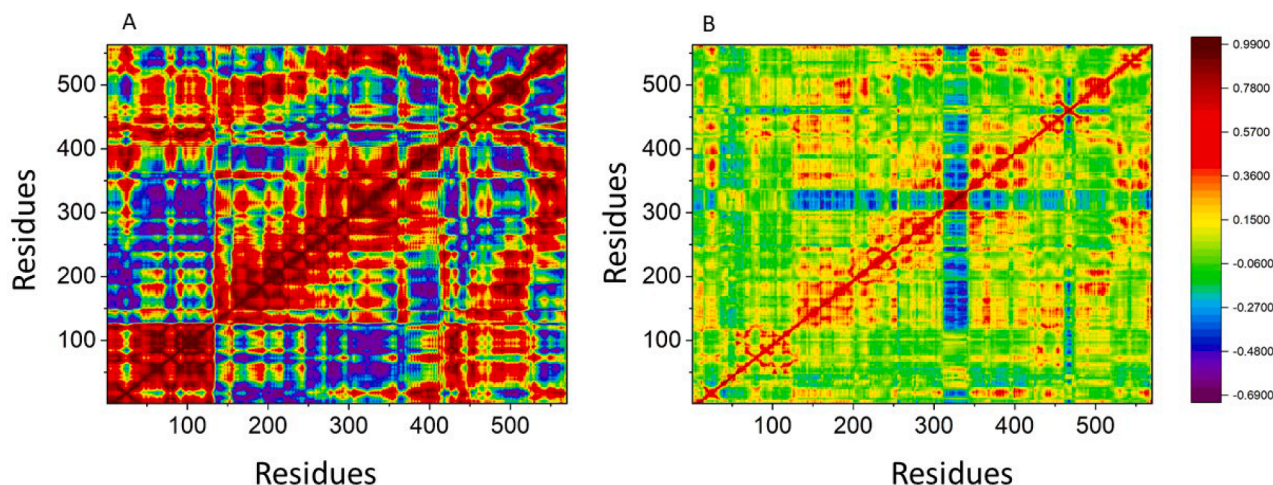


Fig. 5. DCCM analysis of Compound 2j-Urease (A) and aceto-hydroxamic acid-urease (B). The number of residues are shown on X and Y axis.

139.4, 138.4, 138.0, 134.3, 132.7, 132.1, 130.2, 130.2, 129.6, 128.1, 128.0, 120.6, 120.4, 116.9, 112.3, 92.6, 66.7. HREI-MS:  $m/z$  calcd for  $C_{22}H_{18}N_6O_4S$ ,  $[M]^+$  462.1110; Found: 462.1103.

#### 4.2.5. 2-(4-(5-methoxy-1H-benzo[d]imidazol-2-yl)benzoyl)-N-(4-nitrophenyl)hydrazine-1-carbothioamide (1e)

$^1H$ NMR (500 MHz, DMSO- $d_6$ ): 10.7 (s, 1H, NH), 10.2 (s, 1H, NH), 10.1 (s, 1H, NH), 9.8 (s, 1H, NH), 8.3 (d,  $J = 6.8$  Hz, 2H, Aromatic H), 8.0 (m, 2H, Aromatic H), 7.7 (d,  $J = 6.7$  Hz, 2H, Aromatic H), 7.6 (d,  $J = 6.0$  Hz, 2H, Aromatic H), 7.4 (t,  $J = 6.6$  Hz, 1H, Aromatic H), 7.3 (d,  $J = 6.3$  Hz, 1H, Aromatic H), 7.2 (d,  $J = 6.0$  Hz, 1H, Aromatic H), 3.6 (s, 3H, OCH<sub>3</sub>);  $^{13}C$ NMR (125 MHz, DMSO- $d_6$ ):  $\delta$  184.6, 165.2, 157.0, 153.6, 144.6, 139.4, 137.8, 133.8, 132.4, 130.1, 130.0, 128.2, 128.2, 124.8, 124.8, 124.1, 124.0, 119.2, 112.4, 80.5, 66.33. HREI-MS:  $m/z$  calcd for  $C_{22}H_{18}N_6O_4S$ ,  $[M]^+$  462.1110; Found: 462.1105.

#### 4.2.6. N-(4-fluorophenyl)-2-(4-(5-methoxy-1H-benzo[d]imidazol-2-yl)benzoyl)hydrazine-1-carbothioamide (1f)

$^1H$ NMR (500 MHz, DMSO- $d_6$ ): 10.6 (s, 1H, NH), 10.5 (s, 1H, NH), 9.78 (s, 1H, NH), 9.70 (s, 1H, NH), 8.3 (d,  $J = 6.8$  Hz, 2H, Aromatic H), 8.2 (d,  $J = 6.6$  Hz, 2H, Aromatic H), 8.1 (t,  $J = 6.5$  Hz, 1H, Aromatic H), 7.7 (d,  $J = 6.2$  Hz, 2H, Aromatic H), 7.5 (m, 3H, Aromatic H), 7.3 (d,  $J = 6.4$  Hz, 1H, Aromatic H), 3.6 (s, 3H, OCH<sub>3</sub>);  $^{13}C$ NMR (125 MHz, DMSO- $d_6$ ):  $\delta$  184.2, 165.1, 164.2, 156.9, 153.1, 139.8, 137.9, 134.0, 133.9, 132.4, 132.1, 132.1, 130.0, 130.0, 126.9, 126.8, 119.8, 115.6, 115.6, 111.9, 80.3, 66.8. HREI-MS:  $m/z$  calcd for  $C_{22}H_{18}FN_5O_2S$ ,  $[M]^+$  435.1165; Found: 435.1156.

#### 4.2.7. N-(2,3-dichlorophenyl)-2-(4-(5-methoxy-1H-benzo[d]imidazol-2-yl)benzoyl)hydrazine-1-carbothioamide (1g)

$^1H$ NMR (500 MHz, DMSO- $d_6$ ): 10.6 (s, 1H, NH), 9.9 (s, 1H, NH), 9.5 (s, 1H, NH), 8.2 (d,  $J = 7.1$  Hz, 2H, Aromatic H), 8.0 (m, 2H, Aromatic H), 7.7 (d,  $J = 6.2$  Hz, 1H, Aromatic H), 7.6 (d,  $J = 6.1$  Hz, 2H, Aromatic H), 7.5 (t,  $J = 6.0$  Hz, 1H, Aromatic H), 7.3 (d,  $J = 6.9$  Hz, 1H, Aromatic H), 7.2 (m, 1H, Aromatic H), 3.6 (s, 3H, OCH<sub>3</sub>);  $^{13}C$ NMR (125 MHz, DMSO- $d_6$ ):  $\delta$  184.5, 165.4, 157.1, 153.2, 139.8, 138.4, 137.8, 135.8, 134.2, 133.4, 132.6, 132.0, 132.0, 131.9, 130.2, 128.2, 127.9, 127.8, 120.1, 112.2, 79.9, 66.7. HREI-MS:  $m/z$  calcd for  $C_{22}H_{17}Cl_2N_5O_2S$ ,  $[M]^+$  485.0840; Found: 485.0833.

#### 4.2.8. N-(3,4-dichlorophenyl)-2-(4-(5-methoxy-1H-benzo[d]imidazol-2-yl)benzoyl)hydrazine-1-carbothioamide (1h)

$^1H$ NMR (500 MHz, DMSO- $d_6$ ): 10.6 (s, 1H, NH), 10.4 (s, 1H, NH), 9.9 (s, 1H, NH), 9.0 (s, 1H, NH), 8.2 (d,  $J = 6.7$  Hz, 2H, Aromatic H), 8.1 (d,  $J = 6.2$  Hz, 2H, Aromatic H), 7.9 (s, 1H, Aromatic H), 7.7 (d,  $J = 6.3$  Hz, 1H, Aromatic H), 7.5 (m, 2H, Aromatic H), 7.3 (d,  $J = 6.6$  Hz, 1H, Aromatic H), 7.1 (t,  $J = 6.7$  Hz, 1H, Aromatic H), 3.6 (s, 3H, OCH<sub>3</sub>);  $^{13}C$ NMR (125 MHz, DMSO- $d_6$ ):  $\delta$  183.9, 165.2, 156.5, 153.0, 139.8, 137.6, 136.8, 134.9, 133.9, 133.1, 132.1, 130.0, 130.0, 129.9, 128.9, 126.3, 126.2, 121.6, 119.3, 112.0, 80.5, 66.7. HREI-MS:  $m/z$  calcd for  $C_{22}H_{17}Cl_2N_5O_2S$ ,  $[M]^+$  485.0480; Found: 485.0475.

#### 4.2.9. N-(2,6-dimethylphenyl)-2-(4-(5-methoxy-1H-benzo[d]imidazol-2-yl)benzoyl)hydrazine-1-carbothioamide (1i)

$^1H$ NMR (500 MHz, DMSO- $d_6$ ): 10.6 (s, 1H, NH), 9.5 (s, 1H, NH), 9.3 (s, 1H, NH), 8.3 (d,  $J = 6.7$  Hz, 2H, Aromatic H), 8.1 (d,  $J = 6.8$  Hz, 2H, Aromatic H), 7.8 (d,  $J = 6.4$  Hz, 1H, Aromatic H), 7.6 (d,  $J = 6.0$  Hz, 1H, Aromatic H), 7.4 (m, 3H, Aromatic H), 7.2 (d,  $J = 6.2$  Hz, 1H, Aromatic H), 3.6 (s, 3H, OCH<sub>3</sub>), 2.6 (s, 6H, CH<sub>3</sub>);  $^{13}C$ NMR (125 MHz, DMSO- $d_6$ ):  $\delta$  183.8, 165.5, 156.7, 153.2, 140.0, 137.7, 136.4, 135.2, 135.2, 134.6, 132.6, 130.1, 130.1, 128.4, 128.3, 126.9, 126.8, 125.8, 119.6, 111.8, 81.9, 67.0, 18.6, 18.6. HREI-MS:  $m/z$  calcd, for  $C_{24}H_{23}N_5O_2S$ ,  $[M]^+$  445.1572; Found: 445.1586.

#### 4.2.10. 2-(4-(5-methoxy-1H-benzo[d]imidazol-2-yl)benzoyl)-N-(p-tolyl)hydrazine-1-carbothioamide (1j)

$^1H$ NMR (500 MHz, DMSO- $d_6$ ): 10.58 (s, 1H, NH), 10.2 (s, 1H, NH), 9.7 (s, 1H, NH), 9.5 (s, 1H, NH), 8.3 (d,  $J = 6.6$  Hz, 2H, Aromatic H), 8.1 (m, 4H, Aromatic H), 7.7 (t,  $J = 6.2$  Hz, 1H, Aromatic H), 7.5 (m, 4H, Aromatic H), 7.3 (d,  $J = 6.5$  Hz, 1H, Aromatic H), 7.2 (d,  $J = 6.1$  Hz, 1H, Aromatic H), 3.6 (s, 3H, OCH<sub>3</sub>);  $^{13}C$ NMR (125 MHz, DMSO- $d_6$ ):  $\delta$  182.8, 165.5, 156.8, 153.1, 139.7, 139.6, 136.7, 136.4, 134.4, 132.6, 130.0, 130.0, 128.9, 128.8, 128.2, 128.1, 127.3, 127.3, 127.3, 120.1, 112.3, 79.8, 67.9, 22.6. HREI-MS:  $m/z$  calcd for  $C_{23}H_{21}N_5O_2S$ ,  $[M]^+$  431.1416; Found: 431.1411

#### 4.2.11. 4-(4-(5-methoxy-1H-benzo[d]imidazol-2-yl)benzoyl)-N-methylhydrazine-1-carbothioamide (1k)

$^1H$ NMR (500 MHz, DMSO- $d_6$ ): 13.3 (s, 1H, NH), 13.0 (s, 1H, NH), 9.8 (s, 1H, NH), 9.7 (s, 1H, NH), 8.2 (d,  $J = 6.9$  Hz, 2H, Aromatic H), 8.0 (m, 2H, Aromatic H), 7.7 (d,  $J = 6.2$  Hz, 1H, Aromatic H), 7.5 (d,  $J = 6.0$  Hz, 1H, Aromatic H), 7.2 (d,  $J = 6.4$  Hz, 1H, Aromatic H), 3.6 (s, 3H, OCH<sub>3</sub>), 2.9 (s, 3H, CH<sub>3</sub>);  $^{13}C$ NMR (125 MHz, DMSO- $d_6$ ):  $\delta$  183.9, 165.2, 157.0, 152.8, 139.8, 137.7, 135.2, 132.6, 129.9, 129.8, 127.8, 127.8, 119.6, 111.9, 83.5, 68.1, 35.6. HREI-MS:  $m/z$  calcd for  $C_{17}H_{17}N_5O_2S$ ,  $[M]^+$  355.1103; Found: 355.1197

#### 4.2.12. 2-bromo-N'-(4-(5-methoxy-1H-benzo[d]imidazol-2-yl)benzoyl)benzenesulfonohydrazide (2a)

$^1H$ NMR (500 MHz DMSO- $d_6$ )  $\delta$  10.87 (s, 1H, NH), 10.04 (s, 1H, NH), 8.24 (d,  $J = 6.5$  Hz, 2H, Aromatic), 8.01 (d,  $J = 6.5$  Hz, 2H, Aromatic), 7.85 (d,  $J = 6.2$  Hz, 1H, Aromatic), 7.79 (t,  $J = 6.1$  Hz, 1H, Aromatic), 7.72 (d,  $J = 6.2$  Hz, 1H, Aromatic), 7.59 (t,  $J = 6.0$  Hz, 1H, Aromatic), 7.56 (d,  $J = 6.8$  Hz, 1H, Aromatic), 7.20 (s, 1H, Aromatic), 7.05 (d,  $J = 6.8$  Hz, 1H, Aromatic), 3.82 (s, 3H, O—CH<sub>3</sub>),  $^{13}C$ NMR (125 MHz DMSO- $d_6$ )  $\delta$  163.3, 153.2, 150.3, 145.9, 139.2, 138.1, 135.6, 134.0, 133.7, 131.1, 130.2, 130.2, 129.4, 128.3, 127.7, 127.7, 119.3, 117.2, 111.4, 103.3, 41.3. HREI-MS:  $m/z$  calcd for  $C_{21}H_{17}BrN_4O_4S$ ,  $[M]^+$  500.0154; Found: 500.0143

#### 4.2.13. 4-bromo-N'-(4-(5-methoxy-1H-benzo[d]imidazo2yl)benzoyl)benzenesulfonohydrazide (2b)

$^1H$ NMR (500 MHz DMSO- $d_6$ )  $\delta$  10.88 (s, 1H, NH), 10.03 (s, 1H, NH), 8.23 (d,  $J = 6.2$  Hz, 2H, Aromatic), 7.93 (d,  $J = 6.2$  Hz, 2H, Aromatic), 7.89 (d,  $J = 5.2$  Hz, 2H, Aromatic), 7.82 (d,  $J = 5.4$  Hz, 2H, Aromatic), 7.56 (d,  $J = 5.8$  Hz, 1H, Aromatic), 7.29 (s, 1H, Aromatic), 6.88 (d,  $J = 5.7$  Hz, 1H, Aromatic), 3.82 (s, 3H, O—CH<sub>3</sub>),  $^{13}C$ NMR (125 MHz DMSO- $d_6$ )  $\delta$  164.9, 152.6, 151.4, 139.1, 138.5, 137.3, 133.3, 132.1, 131.9, 131.9, 130.6, 130.6, 129.4, 129.4, 127.4, 127.4, 126.2, 121.7, 113.4, 103.7, 41.6. HREI-MS:  $m/z$  calcd for  $C_{21}H_{17}BrN_4O_4S$ ,  $[M]^+$  500.0154; Found: 500.0144

#### 4.2.14. 2-chloro-N'-(4-(5-methoxy-1H-benzo[d]imidazol-2-yl)benzoyl)benzenesulfonohydrazide (2c)

$^1H$ NMR (500 MHz DMSO- $d_6$ )  $\delta$  10.81 (s, 1H, NH), 10.10 (s, 1H, NH), 8.29 (d,  $J = 6.75$  Hz, 2H, Aromatic), 7.98 (d,  $J = 7.4$  Hz, 2H, Aromatic), 7.84 (d,  $J = 6.6$  Hz, 1H, Aromatic), 7.65 (d,  $J = 5.7$  Hz, 2H, Aromatic), 7.49 (d,  $J = 6.3$  Hz, 1H, Aromatic), 7.30 (m, 2H, Aromatic), 7.22 (s, 1H, Aromatic), 6.88 (d,  $J = 6.5$  Hz, 1H, Aromatic), 3.91 (s, 3H, O—CH<sub>3</sub>),  $^{13}C$ NMR (125 MHz DMSO- $d_6$ )  $\delta$  165.0, 152.1, 151.2, 144.7, 139.1, 137.6, 134.3, 133.8, 131.7, 131.0, 130.8, 130.3, 130.3, 128.9, 127.2, 127.2, 127.1, 124.8, 114.9, 104.1, 41.6. HREI-MS:  $m/z$  calcd for  $C_{21}H_{17}ClN_4O_4S$ ,  $[M]^+$  441.0424; Found: 441.0424

#### 4.2.15. 4-chloro-N'-(4-(5-methoxy-1H-benzo[d]imidazol-yl)benzoyl)benzenesulfonohydrazide (2d)

$^1H$ NMR (500 MHz DMSO- $d_6$ )  $\delta$  10.79 (s, 1H, NH), 10.13 (s, 1H, NH), 8.34 (d,  $J = 7.0$  Hz, 2H, Aromatic), 7.98 (d,  $J = 6.9$  Hz, 2H, Aromatic), 7.78 (d,  $J = 6.4$  Hz, 2H, Aromatic), 7.69 (d,  $J = 6.2$  Hz, 2H, Aromatic), 7.64 (d,  $J = 6.3$  Hz, 1H, Aromatic), 7.58 (d,  $J = 6.9$  Hz, 1H, Aromatic),



7.09 (s, 1H, Aromatic), 6.88 (d,  $J = 6.8$  Hz, 1H, Aromatic), 3.76 (s, 3H, O—CH<sub>3</sub>), <sup>13</sup>CNMR (125 MHz DMSO-*d*<sub>6</sub>)  $\delta$  165.2, 152.4, 151.2, 141.1, 139.1, 134.8, 134.1, 133.5, 130.8, 130.8, 129.4, 129.4, 128.9, 128.2, 128.2, 127.4, 127.4, 121.5, 114.9, 104.6, 41.8. HREI-MS:  $m/z$  calcd for C<sub>21</sub>H<sub>17</sub>ClN<sub>4</sub>O<sub>4</sub>S, [M]<sup>+</sup> 441.0424; Found: 41.0418

#### 4.2.16. *N'*-(4-(5-methoxy-1H-benzo[d]imidazol-2-yl)benzoyl)-4-nitrobenzenesulfonohydrazide (2e)

<sup>1</sup>HNMR (500 MHz DMSO-*d*<sub>6</sub>)  $\delta$  10.85 (s, 1H, NH), 10.09 (s, 1H, NH), 8.39 (d,  $J = 7.1$  Hz, 2H, Aromatic), 8.29 (d,  $J = 6.6$  Hz, 2H, Aromatic), 8.07 (d,  $J = 7.2$  Hz, 2H, Aromatic), 8.00 (d,  $J = 6.3$  Hz, 2H, Aromatic), 7.59 (d,  $J = 6.1$  Hz, 2H, Aromatic), 7.24 (s, 1H, Aromatic), 6.95 (d,  $J = 6.1$  Hz, 1H, Aromatic), 3.91 (s, 3H, O—CH<sub>3</sub>), <sup>13</sup>CNMR (125 MHz DMSO-*d*<sub>6</sub>)  $\delta$  166.3, 151.4, 151.5, 151.1, 145.3, 139.3, 138.6, 135.5, 132.1, 131.1, 131.1, 129.4, 129.4, 127.8, 127.8, 124.6, 124.6, 123.3, 113.7, 104.6, 41.9. HREI-MS:  $m/z$  calcd for C<sub>21</sub>H<sub>17</sub>N<sub>5</sub>O<sub>6</sub>S, [M]<sup>+</sup> 467.0900; Found: 467.0908

#### 4.2.17. *N'*-(4-(5-methoxy-1H-benzo[d]imidazol-2-yl)benzoyl)-2,4-dinitrobenzenesulfonohydrazide (2f)

<sup>1</sup>HNMR (500 MHz DMSO-*d*<sub>6</sub>)  $\delta$  10.91 (s, 1H, NH), 10.14 (s, 1H, NH), 8.93 (s, 1H, Aromatic), 8.73 (d,  $J = 7.6$  Hz, 1H, Aromatic), 8.32 (d,  $J = 7.5$  Hz, 2H, Aromatic), 8.29 (d,  $J = 6.3$  Hz, 2H, Aromatic), 7.99 (d,  $J = 6.3$  Hz, 2H, Aromatic), 7.61 (d,  $J = 6.1$  Hz, 1H, Aromatic), 7.24 (s, 1H, Aromatic), 6.95 (d,  $J = 6.1$  Hz, 1H, Aromatic), 3.91 (s, 3H, O—CH<sub>3</sub>), <sup>13</sup>CNMR (125 MHz DMSO-*d*<sub>6</sub>)  $\delta$  164.7, 153.2, 152.4, 151.9, 149.5, 140.5, 139.3, 138.6, 135.2, 132.6, 131.6, 131.6, 130.5, 129.9, 127.8, 127.8, 123.3, 116.4, 113.7, 104.9, 41.9. HREI-MS:  $m/z$  calcd for C<sub>21</sub>H<sub>16</sub>N<sub>6</sub>O<sub>8</sub>S, [M]<sup>+</sup> 512.0750; Found: 512.0742

#### 4.2.18. *N'*-(4-(5-methoxy-1H-benzo[d]imidazol-2-yl)benzoyl)-3-nitrobenzenesulfonohydrazide (2g)

<sup>1</sup>HNMR (500 MHz DMSO-*d*<sub>6</sub>)  $\delta$  10.91 (s, 1H, NH), 10.08 (s, 1H, NH), 8.48 (d,  $J = 7.3$  Hz, 1H, Aromatic), 8.44 (s, 1H, Aromatic), 8.24 (d,  $J = 6.7$  Hz, 2H, Aromatic), 8.22 (d,  $J = 7.3$  Hz, 2H, Aromatic), 7.92 (d,  $J = 6.5$  Hz, 2H, Aromatic), 7.89 (t,  $J = 7.1$  Hz, 1H, Aromatic), 7.55 (d,  $J = 6.1$  Hz, 1H, Aromatic), 7.16 (s, 1H, Aromatic), 6.91 (d,  $J = 6.3$  Hz, 1H, Aromatic), 3.88 (s, 3H, O—CH<sub>3</sub>), <sup>13</sup>CNMR (125 MHz DMSO-*d*<sub>6</sub>)  $\delta$  165.2, 153.4, 151.9, 147.9, 141.3, 140.2, 138.8, 133.5, 132.6, 131.9, 131.5, 131.5, 129.9, 127.9, 127.9, 127.2, 123.3, 121.2, 116.6, 105.4, 42.0. HREI-MS:  $m/z$  calcd for C<sub>21</sub>H<sub>17</sub>N<sub>5</sub>O<sub>6</sub>S, [M]<sup>+</sup> 467.0907; Found: 467.0900

#### 4.2.19. 4-methoxy-*N'*-(4-(5-methoxy-1H-benzo[d]imidazol-2-yl)benzoyl)benzenesulfonohydrazide (2h)

<sup>1</sup>HNMR (500 MHz DMSO-*d*<sub>6</sub>)  $\delta$  10.19 (s, 1H, NH), 9.76 (s, 1H, NH), 8.01 (d,  $J = 6.8$  Hz, 2H, Aromatic), 7.88 (d,  $J = 6.6$  Hz, 2H, Aromatic), 7.71 (d,  $J = 6.2$  Hz, 2H, Aromatic), 7.57 (d,  $J = 6.1$  Hz, 2H, Aromatic), 7.10 (s, 1H, Aromatic), 7.04 (d,  $J = 6.5$  Hz, 2H, Aromatic), 6.84 (d,  $J = 6.1$  Hz, 1H, Aromatic), 3.84 (s, 3H, O—CH<sub>3</sub>), 3.75 (s, 3H, O—CH<sub>3</sub>), <sup>13</sup>CNMR (125 MHz DMSO-*d*<sub>6</sub>)  $\delta$  163.8, 163.5, 152.3, 151.1, 139.1, 138.2, 133.2, 132.4, 129.8, 129.8, 129.0, 127.7, 127.7, 127.0, 127.0, 121.43, 117.5, 117.5, 114.6, 104.5, 41.3, 41.3. HREI-MS:  $m/z$  calcd for C<sub>22</sub>H<sub>20</sub>N<sub>4</sub>O<sub>5</sub>S, [M]<sup>+</sup> 452.1154; Found: 452.1148

#### 4.2.20. *N'*-(4-(5-methoxy-1H-benzo[d]imidazol-2-yl)benzoyl)-2-methylnitrobenzenesulfonohydrazide (2i)

<sup>1</sup>HNMR (500 MHz DMSO-*d*<sub>6</sub>)  $\delta$  10.87 (s, 1H, NH), 10.11 (s, 1H, NH), 8.61 (s, 1H, Aromatic), 8.60 (d,  $J = 7.1$  Hz, 1H, Aromatic), 8.35 (d,  $J = 6.9$  Hz, 2H, Aromatic), 8.26 (d,  $J = 6.4$  Hz, 2H, Aromatic), 7.92 (d,  $J = 6.5$  Hz, 2H, Aromatic), 7.85 (d,  $J = 6.4$  Hz, 2H, Aromatic), 7.57 (d,  $J = 6.2$  Hz, 2H, Aromatic), 7.24 (s, 1H, Aromatic), 6.94 (d,  $J = 6.3$  Hz, 1H, Aromatic), 3.86 (s, 3H, OCH<sub>3</sub>), <sup>13</sup>CNMR (125 MHz DMSO-*d*<sub>6</sub>)  $\delta$  165.4, 152.6, 151.0, 145.0, 144.2, 140.3, 139.8, 138.6, 134.0, 132.2, 130.2, 129.4, 129.4, 128.0, 127.3, 127.3, 124.2, 121.1, 111.9, 103.6, 41.3, 20.4. HREI-MS:  $m/z$  calcd for C<sub>22</sub>H<sub>19</sub>N<sub>5</sub>O<sub>6</sub>S, [M]<sup>+</sup> 481.1056; Found:

481.1049

#### 4.2.21. 2,4-difluoro-*N'*-(4-(5-methoxy-1H-benzo[d]imidazol-2-yl)benzoyl)benzenesulfonohydrazide (2j)

<sup>1</sup>HNMR (500 MHz DMSO-*d*<sub>6</sub>)  $\delta$  10.85 (s, 1H, NH), 10.09 (s, 1H, NH), 8.25 (d,  $J = 6.8$  Hz, 2H, Aromatic), 7.91 (d,  $J = 6.7$  Hz, 2H, Aromatic), 7.74 (d,  $J = 6.4$  Hz, 1H, Aromatic), 7.56 (d,  $J = 6.2$  Hz, 1H, Aromatic), 7.32 (d,  $J = 6.4$  Hz, 2H, Aromatic), 7.24 (s, 1H, Aromatic), 7.11 (s, 1H, Aromatic), 6.94 (d,  $J = 6.1$  Hz, 1H, Aromatic), 3.91 (s, 3H, OCH<sub>3</sub>), <sup>13</sup>CNMR (125 MHz DMSO-*d*<sub>6</sub>)  $\delta$  165.1, 163.3, 159.2, 152.7, 151.2, 139.4, 138.8, 135.1, 132.2, 131.3, 131.3, 130.5, 127.3, 127.3, 122.5, 121.1, 114.5, 111.7, 105.0, 104.3. 41.9. HREI-MS:  $m/z$  calcd for C<sub>21</sub>H<sub>16</sub>F<sub>2</sub>N<sub>4</sub>O<sub>4</sub>S, [M]<sup>+</sup> 458.0860; Found: 458.0857

### 4.3. Urease assay protocol

*In-vitro* urease tests for the synthesized compounds were carried out by using the previously described approach with slight modification [42].

### 4.4. Cytotoxicity test

All synthesized analogs were verified and originated nontoxic, the comprehensive protocol was used as reported by our group [43].

### 4.5. Docking studies protocol

The molecular docking analysis was carried out using the Molecular Operating Environment (MOE) software tool [44–47] to investigate the binding mechanism of the synthesized compounds against the urease enzyme. First the 3D structural coordinates of the synthesized molecules were built using a molecular module. Then, using the default MOE settings (gradient: 0.05, Force Field: MMFF94X), all of the compounds were protonated and energy was reduced. The target enzyme's 3D structure was obtained from the RCSB database using PDB code 4UBP. Once, all the water molecules from the enzyme have been eliminated. After 3D protonation, we reduced the energy using the default MOE software parameters in order to get a stable conformation. After removing all of the water molecules from the enzyme we have used the default parameters of the MOE program for energy minimization after 3D protonation to obtain a stable conformation. The default parameters of MOE program were employed for docking studies, i.e., Placement: Tri-angle Matcher, rescoring 1: London dG, Refinement: Force field, and rescoring 2: GBVI/WSA. Total ten conformations were allowed for each ligand, and the top-ranked conformations based on docking score were chosen for further investigation.

### 4.6. MD simulation study

The Amber 22 package was used for the MD simulations of the complexes. The initial systems preparation was done using the Amber tleap module. The two-force field such as FF14SB and GAFF were used for protein and ligand respectively. The protein-ligand complexes were immersed into an 10 Å TIP3P hydrated cubic box. The counter ions such as chloride or sodium were added to the system to neutralize the charges [40]. Under periodic boundary conditions, energy minimization, heat, density and equilibration were carried out. At 310 K, the final production step of 200 ns was completed for each system. Following the successful completion of the 200 ns MD simulation post simulation analysis such as RMSD, RMSF and DCCM were carried out using the CPPTRAJ package of Amber 22 software [48].

### CRedit authorship contribution statement

Abdullah Yahya Abdullah Alzahrani: Software, Visualization. Bushra Adalat: Methodology. Hayat Ullah: Conceptualization, Writing

– original draft. **Muhammad Taha:** Formal analysis. **Mohamed S. Othman:** Writing – review & editing. **Mohamed A. Fareid:** Writing – review & editing. **Azza M. Khaled:** Writing – review & editing. **Fazal Rahim:** Supervision, Writing – original draft.

### Declaration of Competing Interest

The authors declare that they have no known competing financial interests or personal relationships that could have appeared to influence the work reported in this paper.

### Data availability

The data that has been used is confidential.

### Acknowledgment

This research was funded by Scientific Research Deanship at University of Ha'il—Saudi Arabia through project number RG-23 084.

### References

- [1] P.E. Wilcox, Chymotrypsinogens—chymotrypsins, *Method. Enzymol* 19 (1970) 64–108.
- [2] M.E. Cuff, K.I. Miller, K.E. van Holde, W.A. Hendrickson, Crystal structure of a functional unit from Octopus hemocyanin, *J. Mol. Biol.* 278 (1998) 855–870.
- [3] R.H. Holm, P. Kennepohl, E.I. Solomon, Structural and functional aspects of metal sites in biology, *Chem. Rev.* 96 (1996) 2239–2314.
- [4] S. Schindler, Reactivity of copper(I) Complexes towards dioxygen, *Eur. J. Inorg. Chem.* (2000) 2311–2326.
- [5] A. Coblenz, Treatment of geriatric peptic ulcer with chymotrypsin and an antibiotic, *J. Am. Geriatr. Soc.* 16 (9) (1968) 1039–1046.
- [6] H. Ullah, F. Rahim, E. Ullah, S. Hayat, Z. Rehman, S.A.A. Shah, Synthesis, in vitro  $\alpha$ -glucosidase activity and in silico molecular docking study of Isatin Analogues, *Chem. Data Collect.* 43 (2023), 100987.
- [7] R. Walia, H. Md, S.F. Naaz, K. Iqbal, H.S. Lamba, Benzimidazole derivatives—an overview, *Int. J. Res. Pharm. Chem.* 1 (2011) 565.
- [8] H. Ullah, M. Jabeen, F. Rahim, A. Hussain, I. Uddin, M.U. Khan, M. Nabi, Synthesis, acetylcholinesterase and butyrylcholinesterase inhibitory potential and molecular docking study of thiazole bearing thiourea analogues, *Chem. Data Collect.* 44 (2023), 100988.
- [9] V.K. Forstová, J. Lamka, V. Cvilink, V. Hanušová, L. Skálová, Factors affecting pharmacokinetics of benzimidazole anthelmintics in food-producing animals: the consequences and potential risks, *Res. Vet. Sci.* 91 (2011) 333.
- [10] H. Ullah, N. Ahmad, F. Rahim, I. Uddin, I.U. Khan, A. Rehman, A. Wadood, Synthesis, molecular docking study of thiazole derivatives and exploring their dual inhibitor potentials against  $\alpha$ -amylase and  $\alpha$ -glucosidase, *Chem. Data Collect.* 41 (2022), 100932.
- [11] R.K. Ujjinamatada, A. Baier, P. Borowski, R.S. Hosmane, An analogue of AICAR with dual inhibitory activity against WNV and HCV NTPase/helicase: synthesis and in vitro screening of 4-carbamoyl-5-(4,6-diamino-2,5-dihydro-1,3,5-triazin-2-yl)imidazole-1-beta-D-ribofuranoside, *Bioorg. Med. Chem. Lett.* 17 (2007) 2285.
- [12] S. Khan, H. Ullah, F. Rahim, M. Taha, S.A.A. Shah, K.M. Khan, New thiazole-based thiazolidinone derivatives: synthesis, in vitro  $\alpha$ -amylase,  $\alpha$ -glucosidase activities and silico molecular docking study, *Chem. Data Collect.* 42 (2022), 100967.
- [13] J.R. Kumar, L. Jawahar, D.P. Pathak, Synthesis of benzimidazole derivatives: as anti-hypertensive agents, *J. Chem.* 3 (2006) 278.
- [14] H. Zada, H. Ullah, S. Hayat, F. Rahim, F. Khan, A. Wadood, Synthesis of triazinoindole bearing sulfonamide derivatives, in vitro  $\alpha$ -amylase activity and their molecular docking study, *Chem. Data Collect.* 39 (2022), 100875.
- [15] H. Ullah, F. Rahim, M. Taha, R. Hussain, Z. Wahab, G.A. Miana, K.M. Khan, Aryloxadiazole Schiff bases: synthesis,  $\alpha$ -glucosidase in vitro inhibitory activity and their in silico studies, *Arab. J. Chem.* 13 (2020) 4904–4915.
- [16] X.J. Wang, M.Y. Xi, J.H. Fu, F.R. Zhang, G.F. Cheng, D.L. Yin, Q.D. You, Synthesis, biological evaluation and SAR studies of benzimidazole derivatives as H1-antihistamine agents, *Chin. Chem. Lett.* 23 (2012) 707.
- [17] Z.S. Saify, A. Kamil, S. Akhtar, M. Taha, A. Khan, K.M. Khan, S. Jahan, F. Rahim, S. Perveen, M.I. Choudhary, 2-(2-Pyridyl) benzimidazole derivatives and their urease inhibitory activity, *Med. Chem. Res.* 23 (2014) 4447.
- [18] F. Rahim, H. Ullah, M.T. Javid, A. Wadood, M. Taha, M. Ashraf, A. Shaikat, M. Junaid, S. Hussain, W. Rehman, R. Mehmood, M. Sajid, M.N. Khan, K.M. Khan, Synthesis, in vitro evaluation and molecular docking studies of thiazole derivatives as new inhibitors of  $\alpha$ -glucosidase, *Bioorg. Chem.* 62 (2015) 15–21.
- [19] G. Chen, Z. Liu, Y. Zhang, X. Shan, L. Jiang, Y. Zhao, G. Liang, Synthesis and Anti-inflammatory Evaluation of Novel Benzimidazole and Imidazopyridine Derivatives, *ACS Med. Chem. Lett.* 4 (2012) 69.
- [20] F. Rahim, M.T. Javed, H. Ullah, A. Wadood, M. Taha, S. Mirza, K.M. Khan, Synthesis, molecular docking, acetylcholinesterase and butyrylcholinesterase inhibitory potential of thiazole analogs as new inhibitors for Alzheimer disease, *Bioorg. Chem.* 62 (2015) 106–116.
- [21] D.N. Patagar, S.R. Batakurki, R. Kusanur, S.M. Patra, S. Saravanakumar, M. Ghate, Synthesis, antioxidant and anti-diabetic potential of novel benzimidazole substituted coumarin-3-carboxamides, *J. Mol. Struct.* 1274 (2023), 134589.
- [22] W. Hu, W. Zhou, C. Xia, X. Wen, Synthesis and anticancer activity of thiosemicarbazones, *Bioorg. Med. Chem. Lett.* 16 (2006) 2213–2218.
- [23] X. Du, C. Guo, E. Hansall, P.S. Doyle, J.H. McKerrow, F.E. Cohen, Synthesis and structure-activity relationship study of potent trypanocidal thio semicarbazone inhibitors of the trypanosomal cysteine protease cruzain, *J. Med. Chem.* 45 (2002) 2695.
- [24] D.B. Lovejoy, D.R. Richardson, Novel "hybrid" iron chelators derived from aroylhydrazones and thiosemicarbazones demonstrate selective antiproliferative activity against tumor cells, *Blood* 100 (2002) 666–676.
- [25] A.E. Liberta, D.X. West, Antifungal and antitumor activity of heterocyclic thiosemicarbazones and their metal complexes: current status, *Biomaterials* 5 (1992) 121–126.
- [26] H. Ullah, G. Arshad, F. Rahim, A. Nawaz, A. Samad, A. Wadood, Synthesis, in vitro urease inhibitory potential and molecular docking study of bis-indole bearing sulfonamide analogues, *Chem. Data Collect.* 44 (2023), 100999.
- [27] P. Zajdel, A. Partyka, K. Marciniec, A.J. Bojarski, M. Pawlowski, A. Wesolowska, Quinoline- and isoquinoline-sulfonamide analogs of aripiprazole: novel antipsychotic agents, *Future Med. Chem.* 6 (2014) 57–75.
- [28] S. Mutahir, J. Jończyk, M. Bajda, I.U. Khan, M.A. Khan, N. Ullah, M. Ashraf, S. Riaz, S. Hussain, M. Yar, Novel biphenyl bis -sulfonamides as acetyl and butyrylcholinesterase inhibitors: synthesis, biological evaluation and molecular modeling studies, *Bioorg. Chem.* 64 (2016) 13–20.
- [29] M. Morris, G.M. Knudsen, S. Maeda, J.C. Trinidad, A. Ioanoviciu, A.L. Burlingame, L. Mucke, Tau-post-translational modifications in wild-type and human amyloid precursor protein. Transgenic mice, *Nat. Neurosci.* 18 (2015) 1183–1189.
- [30] H.I. Gul, C. Yamali, H. Sakagami, A. Angeli, J. Leitans, A. Kazaks, K. Tars, D. O. Ozgun, C.T. Supuran, New anticancer drug candidates' sulfonamides as selective hCA IX or hCA XII inhibitors, *Bioorg. Chem.* 77 (2018) 411–419.
- [31] N. Asemanipoor, M. Mohammadi-Khanaposhtani, S. Moradi, M. Vahidi, M. Asadi, M. Ali Faramarzi, M. Mahdavi, M. Biglar, B. Larjani, H. Hamedifar, M. Hamed Hajimiri, Synthesis and biological evaluation of new benzimidazole-1,2,3-triazole hybrids as potential  $\alpha$ -glucosidase inhibitors, *Bioorg. Chem.* 95 (2020), 103482.
- [32] H. Azizian, K. Pedrood, A. Moazzam, Y. Valizadeh, K. Khavanizadeh, A. Zamani, M. Mohammadi-Khanaposhtani, S. Mojtavavi, M.A. Faramarzi, S. Hosseini, Y. Sarrafi, H. Adibi, B. Larjani, H. Rastegar, M. Mahdavi, Molecular dynamic, synthesis, anti- $\alpha$ -glucosidase assessment, and ADMET prediction of new benzimidazole-Schiff base derivatives, *Sci. Rep.* 12 (1) (2022) 14870.
- [33] M. Noori, A. Davoodi, A. Iraj, N. Dastyafteh, M. Khalili, M. Asadi, M. M. Khanaposhtani, S. Mojtavavi, M. Dianatpour, M.A. Faramarzi, B. Larjani, M. Amanlou, M. Mahdavi, Design, synthesis, and in silico studies of quinoline-based-benzimidazole bearing different acetamide derivatives as potent  $\alpha$ -glucosidase inhibitors, *Sci. Rep.* 12 (1) (2022) 14019.
- [34] S. Zareei, M. Mohammadi-Khanaposhtani, M. Adib, M. Mahdavi, P. Taslimi, Sulfonamide-phosphonate hybrids as new carbonic anhydrase inhibitors: in vitro enzymatic inhibition, molecular modeling, and ADMET prediction, *J. Mol. Struct.* 1271 (2023), 134114.
- [35] N. Hosseinzadeh, M.N. Montazer, M. Mohammadi-Khanaposhtani, Y. Valizadeh, M. Amanlou, M. Mahdavi, Rational design, synthesis, docking simulation, and ADMET prediction of novel barbituric-hydrazine-phenoxy-1,2,3-triazole-acetamide derivatives as potent urease inhibitors, *Chem. Select* 8 (3) (2023), e202203297.
- [36] M.S. Asgari, H. Azizian, M.N. Montazer, M. Mohammadi-Khanaposhtani, M. Asadi, S. Sepehri, P.R. Ranjbar, R. Rahimi, M. Biglar, B. Larjani, M. Amanlou, M. Mahdavi, New 1,2,3-triazole-(thio)barbituric acid hybrids as urease inhibitors: design, synthesis, in vitro urease inhibition, docking study, and molecular dynamic simulation, *Arch. Pharm. (Weinheim)* 353 (9) (2020), 2000023.
- [37] M. Biglar, R. Mirzazadeh, M. Asadi, S. Sepehri, Y. Valizadeh, Y. Sarrafi, M. Amanlou, B. Larjani, M. Mohammadi-Khanaposhtani, M. Mahdavi, *Bioorg. Chem.* 95 (2020), 103529.
- [38] B. Adalat, F. Rahim, M. Taha, F.J. Alshamrani, E.H. Anouar, N. Uddin, Z.A. Zakaria, Synthesis of benzimidazole-based analogs as anti Alzheimer's disease compounds and their molecular docking studies, *Molecules* 25 (20) (2020) 4828.
- [39] Z.S. Saify, A. Kamil, S. Akhtar, M. Taha, A. Khan, K.M. Khan, S. Jahan, F. Rahim, S. Perveen, M.I. Choudhary, 2-(2-Pyridyl) benzimidazole derivatives and their urease inhibitory activity, *Med. Chem. Res.* 23 (2014) 4447–4454.
- [40] F. Rahim, K. Zaman, M. Taha, H. Ullah, M. Ghufuran, A. Wadood, K.M. Khan, Synthesis, in vitro  $\alpha$ -glucosidase inhibitory potential of benzimidazole bearing bis-Schiff bases and their molecular docking study, *Bioorg. Chem.* 94 (2020), 103394.
- [41] H. Ullah, H. Ullah, M. Taha, F. Khan, F. Rahim, I. Uddin, S. Mubeen, Synthesis, in vitro  $\alpha$ -amylase activity, and molecular docking study of new benzimidazole derivatives, *Russ. J. Organ. Chem.* 57 (6) (2021) 968–975.
- [42] M.W. Weatherburn, Phenol-hypochlorite reaction for determination of ammonia, *Anal. Chem.* 39 (8) (1967) 971–974.
- [43] T. Arshad, K.M. Khan, N. Rasool, 5-Bromo-2-aryl benzimidazole derivatives as non-cytotoxic potential dual inhibitors of  $\alpha$ -glucosidase and urease enzymes, *Bioorg. Chem.* 72 (2017) 21–31.
- [44] C.C.G Inc, Molecular Operating Environment (MOE), Chemical Computing Group Inc, 2016, 1010 Sherbooke St. West, Suite, 910.
- [45] U. Salar, B. Qureshi, K.M. Khan, M.A. Lodhi, Z. Ul Haq, F.A. Khan, S. Hussain, Aryl hydrazones linked thiazolyl coumarin hybrids as potential urease inhibitors, *J. Iran. Chem. Soc.* 19 (4) (2022) 1221–1238.

- [46] M. Taha, S. Ismail, S. Imran, N.B. Almandil, M. Alomari, F. Rahim, K.M. Khan, Synthesis of new urease enzyme inhibitors as antiulcer drug and computational study, *J. Biomolecul. Struct. Dyn.* (2021) 1–16.
- [47] A.R. Phull, M. Hassan, Q. Abbas, H. Raza, I.U. Haq, S.Y. Seo, S.J. Kim, In vitro, in silico elucidation of antiurease activity, kinetic mechanism and COX-2 inhibitory efficacy of coagulansin A of *Withania coagulans*, *Chem. Biodivers.* 15 (1) (2018), e1700427.
- [48] A. Wadood, A. Ajmal, M. Junaid, A.U. Rehman, R. Uddin, S.S. Azam, A. Ali, Machine learning-based virtual screening for STAT3 anticancer drug target, *Curr. Pharmaceut. Des.* 28 (36) (2022) 3023–3032.